Clim. Past Discuss., 4, 1265–1287, 2008
www.clim-past-discuss.net/4/1265/2008/
© Author(s) 2008. This work is distributed under
the Creative Commons Attribution 3.0 License.

Climate of the Past Discussions

Climate of the Past Discussions is the access reviewed discussion forum of *Climate of the Past*

Modeling sensitivity study of the possible impact of snow and glaciers developing over Tibetan Plateau on Holocene African-Asian summer monsoon climate

L. Jin[1], Y. Peng[1], F. Chen[1], and A. Ganopolski[2]

[1]Key Laboratory of Western China's Environmental Systems (Ministry of Education), Lanzhou University, Lanzhou 730000, China
[2]Potsdam Institute for Climate Impact Research, Potsdam, Germany

Received: 13 October 2008 – Accepted: 14 November 2008 – Published: 11 December 2008

Correspondence to: L. Jin (jinly@lzu.edu.cn)

Published by Copernicus Publications on behalf of the European Geosciences Union.

Abstract

The impacts of various scenarios of snow and glaciers developing over the Tibetan Plateau on climate change in Afro-Asian monsoon region and other regions during the Holocene (9 kyr BP–0 kyr BP) are studied by using the coupled climate model of intermediate complexity, CLIMBER-2. The simulations show that the imposed snow and glaciers over the Tibetan Plateau in the mid-Holocene induce global summer temperature decreases, especially in the northern parts of Europe, Asia, and North America. At the same time, with the imposed snow and glaciers, summer precipitation decreases strongly in North Africa and South Asia as well as northeastern China, while it increases in Southeast Asia and the Mediterranean. For the whole period of Holocene (9 kyr BP–0 kyr BP), the response of vegetation cover to the imposed snow and glaciers cover over the Tibetan Plateau is not synchronous in South Asia and in North Africa, showing an earlier and a more rapid decrease in vegetation cover in North Africa from 9 to 6 kyr BP while it has only minor influence on that in South Asia until 5 kyr BP. Imposed gradually increased snow and glacier cover over the Tibetan Plateau causes temperature increases in South Asia and it decreases in North Africa and Southeast Asia during 6 kyr BP to 0 kyr BP. The precipitation decreases rapidly in North Africa and South Asia while it decreases slowly or unchanged during 6 kyr BP to 0 kyr BP with imposed snow and glacier cover over the Tibetan Plateau. The different scenarios of snow and glacier developing over the Tibetan Plateau would result in differences in variation of temperature, precipitation and vegetation cover in North Africa, South Asia and Southeast Asia. The model results show that the response of climate change in African-Asian monsoon region to snow and glacier cover over the Tibetan Plateau is in the way that the snow and glaciers amplify the effect of vegetation feedback and, hence, further amplify orbital forcing.

1 Introduction

Holocene climate change is one of the focus themes both in paleoclimate modeling and proxy data reconstruction communities. By examining 50 globally distributed paleoclimate records, Mayewski et al. (2004) revealed as many as six periods of significant rapid climate change during the Holocene which were synchronous of the whole Earth. It is suggested that changes in insolation related both to Earth's orbital variations and to solar variability played a central role in the global scale changes in climate of the last 11.5 cal kyr (Mayewski et al., 2004). This insolation driving mechanism in the Holocene climate change is supported by climate modeling experiments of the variation of tropical monsoon climate in North Africa and South Asia (Kutzbach and Guetter, 1986; COHMAP Members, 1988) and of changes in the African-Asian monsoon precipitation (Weber et al., 2004). However, external forcing, e.g., the Earth's orbital variations and the solar variability, can be amplified and modified through a number of feedbacks within the climate system leading to marked climate variations in the Holocene (Foley et al., 1994; TEMPO Members, 1996; Claussen and Gayler, 1997; Ganopolski et al., 1998b; Wang, 1999). The atmosphere-vegetation feedback is an important amplifying factor of the North Africa's abrupt climate transition from a wet phase to a dry phase starting at around 6 kyr BP (Texier et al., 1997; Claussen et al., 1999). Studies from lake sediment pollen and carbonate records showed the arid phase in South Asia probably started around 5 kyr BP (Maxwell, 2001; Singh, 2002), coinciding with a stepwise weakening of the southwest monsoon (Gupta and Anderson, 2005), which was closely linked to North Atlantic cold spells, e.g., the millennial-scale cold events during 4.6–4.2 kyr BP (Gupta et al., 2003). In addition, it is indicated that the so-called "Megathemal" or "Holocene Optimum" from 8.5–3.0 kyr BP often mentioned in the Chinese Quaternary and paleoclimate community (Huang, 1998; Qin, 2002), as defined by peak precipitation or effective moisture, is asynchronous in eastern Asian monsoon regions, which is related to a general weakening and southward retreat of the East Asian summer monsoon since about 9 kyr BP (An et al., 2000).

The Tibetan Plateau, with a mean elevation of ca 4.5 km above sea level and an area of 2.5×10^6 km^2, is one of the most imposing topographic features in Central Asia and the greatest glaciated areas outside the Polar Regions. The Tibetan Plateau has a profound influence on regional and global atmospheric circulation and is therefore important for our understanding the dynamics of global environmental and climatic change (Ruddiman and Kuzbach, 1989; Molnar and England, 1990; Prell and Kutzbach, 1992; Yanai et al., 1992). Studies of glacier changes during the late Quaternary were conducted over the Tibetan Plateau and significant progress has been made in recent years (Lehmkuhl and Oven, 2005). Earlier study has revealed that there were intervals of glacier advances over the Tibetan Plateau during the Holocene at about 8.2–7.2 kyr BP, 5.8–4.9 kyr BP, 3 kyr BP and 300–450 yr BP, respectively (Lehmkuhl, 1997). Observation from the Dasuopu glacier (28°23′ N, 85°43′ E) (located in the southwestern region of the Tibetan Plateau) shows a gradually increase of snow accumulation from AD 1600 to 1817, and then a significant increase persisted until AD 1880 (Thompson et al., 2000). At another glacier site, the Guliya ice cap (35°17′ N, 81°29′ E) which is located in northwestern region of the Tibetan Plateau and whose records is believed to cover more than 100 000 years, spanning the whole Holocene to the last interglacial (Christner et al., 2003) showed a rapid decrease in temperature up to 3∼4°C during the period of 7–5 kyr BP (Thompson et al., 1997; Yao et al., 2000). Glaciers at Nanga Parbat (35°14′15″ N, 74°35′21″ E), north western Himalaya Mountains, expanded during the early to middle Holocene ca. 9.0–5.5 ka (Phillips et al., 2000). Evidence from oxygen isotope records in the Bay of Bengal shows that during early-middle Holocene, the Himalayas experienced at least two significant episodes of aridity and intensified glaciation at 5–4.3 kyr BP and ca. 2 kyr BP (Chauhan, 2003). Recently, evidence based on radiocarbon ages of fossil wood buried in moraines, lichen-dated moraines and tree ring identified three main periods of glacier advances in the southeastern Tibetan Plateau during the late Holocene: around AD 200–600, AD 800–1150, and AD 1400–1920, respectively (Yang et al., 2008). By using a set of data from a fully coupled oce an-atmosphere model (FOAM), Casal et al. (2004) calculated the ice-sheet mass bal-

ance for the Tibetan Plateau for the present day, and for the past simulations, under the insolation forcings at 3 kyr BP, 6 kyr BP, 8 kyr BP and 11 kyr BP. Their result show that the area with positive ice-sheet mass balance expands from 11 kyr BP to 0 kyr BP (Casal et al., 2004, Fig. 11). Both observation and modeling of glacier development over the Tibetan Plateau suggest that the Tibetan Plateau may have experienced a glacier fluctuation during the Holocene. There are different suggestions concerning the controlling factors on glacier expansion over Tibetan Plateau during the Holocene. Thompson et al. (2006) suggest that glacier expansion on the southern and central Tibetan Plateau is driven mainly by variation in monsoonal precipitation that is modulated by precession-driven insolation changes, while Yang et al. (2008) argued that it is the temperature change rather than precipitation change caused by variations of the south Asian summer monsoon that is the controlling factor for glacier fluctuation during the late Holocene.

In a previous model study using CLIMBER-2, Jin et al. (2005) studied the impacts of ice and snow cover over the Tibetan Plateau on Holocene climate change and the simulation results suggest that the snow and glacier environment over the Tibetan Plateau is an important factor for Holocene Africa-Asian monsoon retreating and an amplifier for monsoon regional climate variability. In their transient modeling experiments (Jin et al., 2005), the changes of snow and glaciers over the Tibetan Plateau was set to be simply linear increasing from 9 kyr BP to present. However, the assumption that the snow and glaciers developing on the Tibetan Plateau were in a linear way is not possible the real case as it were due to the complexity of snow and glacier development. Because the different scenarios of snow and glaciers developing on the Tibetan Plateau may have different effects on climate change, here, as a follow-up research of Jin et al. (2005), we conduct a series of sensitivity experiments by using CLIMBER-2 focusing on the impacts of different scenarios of snow and glaciers developing over the Tibetan Plateau on Holocene climate changes in African-Asian monsoon region and other regions.

2 Model and experimental set-up

2.1 The model

The Earth system model of intermediate complexity, CLIMBER-2, used in this study was developed in Potsdam Institute for Climate Impact Research (PIK) in Germany to perform the long-term simulations. The model consists of modules describing atmosphere, ocean, sea ice, and terrestrial vegetation. The model of the atmosphere is based on the statistical-dynamical approach and explicitly resolves the large-scale circulation patterns such as subtropical jet streams, Hadley, Ferrel and polar cells, monsoon and centers of action of the Siberian high-pressure area and the Aleutian low-pressure area. It does not resolve individual synoptic weather systems but rather predicts their statistical characteristics, including the fluxes of heat, moisture, and momentum associated with ensembles of synoptic systems. The vertical structure includes a planetary boundary layer, a free troposphere (including cumulus and stratiform clouds) and a stratosphere. Radiative fluxes are computed on 16 vetical levels. The ocean model is a multibasin, zonally averaged model similar to the one used by Stocker et al. (1992), including a model of sea-ice thickness, concentration, and advection. Vertically the ocean is subdivided into 20 uneven layers. Parameterizations for its vorticity balance and Ekman transport are employed. The model of terrestrial vegetation (Brovkin et al., 2002) describe the dynamics of vegetation cover, i.e., fractional coverage of a grid cell by trees, grass, and desert (bare soil), as well as net primary productivity, leaf area index, biomass, and soil carbon pool. Hence, CLIMBER-2 is able to describe changes in vegetation cover that can be interpreted as shifts in vegetation zones smaller than the spatial resolution of the model. Atmosphere and ocean interact through the surface fluxes of heat, fresh water and momentum. The model does not employ flux adjustments. The CLIMBER-2 model has been validated against present-day climate (Petoukhov et al., 2000, 2001; Ganopolski et al., 2001) and has been used successfully for a variety of paleoclimate studies (Ganopolski et al., 1998; Claussen et al., 1999; Jin et al., 2005, 2007).

2.2 The experimental set-up

To mimic various scenarios of snow and glaciers developing over the Tibetan Plateau, five scenarios of snow and glacier area growth over the Tibetan Plateau were set up for the 9 kyr transient simulation, namely ICE0, ICE1, ICE2, ICE3 and ICE4, respectively (see Table 1 for detail).

In all experiments except ICE0, the fraction of snow and glaciers in the grid cell which contain the Tibetan Plateau (30°–40° N, 40°–90° E) in the model is prescribed starting with 0 at 9 kyr BP and ending with 0.2 at 0 kyr BP, with different scenarios of variations of fraction of snow and glaciers over the Tibetan Plateau through 9 kyr BP to 0 kyr BP (See Fig. 1a and Table 1 for a detail).

Three simulations using CLIMBER-2 were conducted for each scenario for snow and glacier area over the Tibetan Plateau for the Holocene. Firstly, the fully coupled atmosphere-ocean-terrestrial vegetation model (AOV) was employed for the transient simulation for the past 9000 years. Secondly, the coupled atmosphere-ocean model (AO) with vegetation cover fixed with 9 kyr BP vegetation as in the equilibrium run at 9 kyr BP was performed. Finally, the simulation AV was run with interactive vegetation (coupled atmosphere-vegetation model), while ocean characteristics were fixed as in the equilibrium run at 9 kyr BP. The AO and AV simulations are intended to investigate interactive effects of ocean and terrestrial vegetation cover, respectively. All transient simulations start from an equilibrium with orbital forcing at 9 kyr BP for 9000 years until present day. The global and seasonal change of the orbital insolation is computed with the algorithm after Berger (1978). No flux corrections between the atmospheric and oceanic modules are applied in the model in any simulation. The atmospheric CO_2 concentration is kept constant at 280 ppmv, and the solar constant is fixed at 1365 W m^{-2}.

3 Results

3.1 Temperature, precipitation and vegetation changes in the last 9 kyr

The transient simulations revealed pronounced responses of CLIMBER-2 to changes in orbital parameters as well as the impacts of snow and glacier cover over the Tibetan Plateau on climate. Figure 1e illustrates that changes in boreal summer temperature in South Asia are quite different from that in Southeast Asia (Fig. 1d) and North Africa (Fig. 1f). Since 6 kyr BP, the summer temperature in South Asia began to increase with the fraction of snow and glacier cover increased over the Tibetan Plateau in all imposed ice scenarios (except for ICE0). The quicker increase of snow and glacier cover over the Tibetan Plateau would cause a faster increase in summer temperature in South Asia, as can be seen when compared scenario ICE4 with ICE1, ICE2, and ICE3 in Fig. 1e. In Southeast Asia and North Africa, the faster increased snow and glacier cover over the Tibetan Plateau leads to an earlier decrease in summer temperature during 8 kyr BP–5 kyr BP, but after 5 kyr BP, even though the snow and glaciers are still growing in all ice scenarios, the summer temperature have a small change (Fig. 1d, f). The summer precipitation in Southeast Asia (Fig. 1g) increases rapidly during the early to mid-Holocene (9 kyr BP to 6 kyr BP) with the gradually increased snow and glacier cover over the Tibetan Plateau, in which the faster the snow and glacier grows (scenario ICE4), the more summer precipitation increases. Since 6 kyr BP, even though the snow and glacier are still growing (scenarios ICE1, ICE2, and ICE3), the summer precipitation in Southeast Asia no more increases or even began to decrease with the fraction of snow and glacier cover over the Tibetan Plateau was kept constant (corresponding to scenario ICE4). In North Africa, the strongest decrease in summer precipitation appears around 5.5–6.5 kyr BP in scenario ICE0 (no-ice) simulation (grey line in Fig. 1i), while in scenarios ICE1 (green), ICE2 (purple), ICE3 (red), and ICE4 (blue), it occurs around 6.5–7.5 kyr BP, 6.5–7.5 kyr BP, 6–7 kyr BP, and 7–8 kyr BP, respectively. In South Asia, including the southern part of the Tibetan Plateau, the rapid and strong reduction in summer precipitation during early to mid-Holocene is

similar to that in North Africa. Compared to scenario ICE0 (no-ice), the ice scenarios (ICE0, ICE1, ICE2, ICE3, and ICE4) show a pronounced increase in summer precipitation in Southeast Asia (Fig. 1g), and a decrease in South Asia (Fig. 1h) and Africa (Fig. 1i). The tendency for the pattern of rapidly increased precipitation in Southeast Asia and decreased in South Asia and North Africa during the early to mid-Holocene may reflect the tendency for the large-scale weakened African-Asian summer monsoon circulation to shift the locus of monsoon rains southeastward (Fig. 2), as a result of the thermal-driving monsoon circulation to be adjusted to the changes in thermal contrast between the African and Eurasian continent and Indian Ocean during the boreal summer, and showing the gradually weakened seasonal cycle of solar insolation in the northern hemisphere began to take into effect, as is also evidenced from the paleoclimate records (Morrill et al., 2003; Tang et al., 2000).

Compared to the changes in near-surface air temperature and precipitation, the fraction f of vegetation cover changed differently. Figure 1b, c shows responses of the changes in the fraction f of vegetation cover to the different scenarios of gradually increased snow and glaciers over the Tibetan Plateau in South Asia and North Africa. In North Africa (Fig. 1c), the vegetation cover decreases earlier and more rapidly than that in South Asia (Fig. 1b) in all imposed ice scenarios. Complete desertification in North Africa appears around 3.5 kyr BP with no-ice imposed over the Tibetan Plateau (scenario ICE0), and by 5.0 kyr BP (scenarios ICE1, ICE2, ICE3), and 6 kyr BP (scenario ICE4), respectively (Fig. 1c), showing a strong feedback effect of snow and glacier cover over the Tibetan Plateau on North African vegetation development. In South Asia, the response of the changes in vegetation cover to the gradually increased snow and glaciers over the Tibetan Plateau lags behind North Africa a few thousand years (the fraction of vegetation cover in South Asia reduces only 10% ($\Delta f \sim -0.1$) for the first 5 kyr for scenarios of ICE1, ICE2, and ICE3) (Fig. 1b), while the fraction of vegetation cover in North Africa reached almost zero at 5 kyr BP (Fig. 1c). The snow and glacier influence on changes of vegetation cover in South Asia began after 5 kyr BP, with a rather rapidly decrease in vegetation cover from 3.5 to 2 kyr BP ($\Delta f \sim -0.35$) in scenar-

ios of ICE1, ICE2, and ICE3. In scenario ICE4, even the snow and glacier cover would not increase any more after 6 kyr BP (Fig. 1a, blue line), its influence last for the rest of the Holocene vegetation evolution compared with scenario ICE0 (Fig. 1b). The simulated fraction of vegetation cover in North Africa are generally coincident with proxy records of changes in vegetation cover evidenced from ocean temperature and terrigenous dust in marine sediment cores off western Africa (deMenocal et al., 2000). The percentage of terrigenous dust contents indicates a dramatic increase in the amount of dust that relates directly to the changes in vegetation as the Sahara expanded across North Africa during 5.7 kyr BP to 5.0 kyr BP (deMenocal et al., 2000).

3.2 Analysis on imposed ice-albedo effect on Holocene climate change in North Africa and South Asia

In order to investigate the synergy of ice-albedo effect with solar insolation and vegetation effects, we performed three other transient simulations AO, AV, AOV with and without imposed snow and glacier cover over the Tibetan Plateau. Figure 3 shows simulated results in North Africa for the last 9000 years from simulations AO, AV, AOV with no-ice scenario ICE0, and with ice scenarios ICE1 and ICE4. About 1 kyr earlier rapidly decrease in near-surface air temperature during the mid-Holocene in ICE4 scenario than in scenario ICE1, and 2 kyr earlier than in scenario ICE0 can be seen in simulations AV and AOV (Fig. 3a, b, c). Similar results are in changes in summer precipitation (Fig. 3d, e, f) and vegetation cover in North Africa (Fig. 3g, h, i). Results of experiments AV and AOV for North Africa show a similar response of CLIMBER-2 to changes in orbital parameters and ice-imposed forcing over the Tibetan Plateau while results of experiment AO show a less variation in all ice-imposed scenarios. It indicates that the effect of snow and glaciers over the Tibetan Plateau could play a role through the vegetation feedbacks, i.e. the ice and snow amplifies the vegetation feedback and the orbital forcing, while the ocean plays only a minor role in North African climate change during the Holocene, as a previous modeling study in work of Claussen et al. (1999).

In South Asia, the imposed effect of snow and glacier forcing over the Tibetan Plateau shows a different impact on summer near-surface air temperature (Fig. 4b, c) and vegetation cover (Fig. 4h, i) compared to that in North Africa (Fig. 3). With a linear increase in snow and glacier cover over the Tibetan Plateau in scenario ICE1, the near surface summer air temperature in South Asia began to increase after around 6 kyr BP in simulations AO, AV, AOV (Fig. 4b), while in North Africa, it still decreases after 6 kyr BP. In scenario ICE4 (Fig. 4c), the near surface summer air temperature in South Asia began to increase almost along with the increase of snow and glacier cover over the Tibetan Plateau at the early Holocene (Fig. 4c). The rapidly increased near surface summer air temperature in South Asia is closely related to the rapid decreases in summer precipitation (Fig. 4e, f) and vegetation cover (Fig. 4h, i) in this region. Figure 4e, f shows that the summer precipitation in South Asia is more sensitive to the effect of snow and glacier cover over the Tibetan Plateau (scenarios ICE1, ICE4) compared to that in no ice scenario (ICE0) (Fig. 4d) in AO, AV, and AOV simulations. Similarly, it is shown that the faster increase in snow and glacier cover over the Tibetan Plateau (scenarios ICE1, ICE4) would cause an earlier (about 1000–2000 years) and rapidly decrease in vegetation cover in South Asia (Fig. 4h, i) compared to that in no-ice scenario (ICE0) (Fig. 4g). The rapid decrease in summer precipitation and in vegetation cover in South Asia is probably responsible for the rapid increase in near surface summer air temperature after 5 kyr BP.

Figure 5a, b shows the simulated differences in sea surface temperatures (SSTs) between 9 kyr BP and 0 kyr BP in simulation AOV without imposed snow and glacier over the Tibetan Plateau (scenario ICE0), indicating a negative SST anomaly in North Indian Ocean (40° E–95° E, 0° N–20° N) in the early Holocene. Figure 5c shows the simulated SST evolution for the last 9 kyr in North Indian Ocean (40° E–95° E, 0° N–20° N), with a slight decrease in SST during the early to mid-Holocene and a gradually increase after 5 kyr BP. It seems that the evolution of near surface summer air temperature in South Asia (Fig. 4b, c) followed the SST evolution in North Indian Ocean (Fig. 5c). However, in no ice scenario (ICE0) experiment, the evolution of summer temperature in South

Asia (Fig. 4a) does not follow the SST evolution in North Indian Ocean (Fig. 5c), indicating that the near surface summer air temperature increase in South Asia after 5 kyr BP can not be attributed to the increase in SST in North Indian Ocean. This is because an increased latent heat flux would release over sea surface and transport to air over continent in South Asia from North Indian Ocean due to increased SST, and hence increases the summer temperature in South Asia, but the increase of evaporation over the ocean and a stronger moisture transport from ocean also increase the cloudiness that may compensate release of latent heat. It is suggested from our modeling experiment that the rapid decrease in precipitation and vegetation cover after 5 kyr BP (Fig. 4e, h) could reduce the albedo of underlying surface in this region, which in return increases the absorbtion of solar radiation and hence increases the temperature.

4 Summary and concluding remarks

Using the climate system model of intermediate complexity, CLIMBER-2, the Holocene climate changes were simulated forced by various scenarios of snow and glaciers developing over the Tibetan Plateau. The simulations show an additional decrease in boreal summer temperature in mid-Holocene (6 kyr BP) when snow and ice glaciers are imposed over the Tibetan Plateau, especially in the northern parts of Europe, Asia, and North America. An increase in snow and glaciers over the Tibetan Plateau for the last 9000 years would lead to an earlier and more rapidly climate change in African-Asian monsoon region as well as the changes in summer temperature in South Asia and summer precipitation in Southeast Asia. The faster the snow and glaciers increase, the earlier the rapid decrease in boreal summer temperature and precipitation as well as vegetation cover in North Africa. However, the faster increase in snow and glaciers over the Tibetan Plateau would cause an increase in near surface summer air temperature in South Asia. The rapid decrease in vegetation in South Asia was lagged behind North Africa about 1.5 to 2.0 kyr. The model results suggest that the vegetation feedback is an important factor for climate variability in North Africa, while the ocean

plays only a minor role.

The surface albedo and latent heat flux must be important in boreal summer temperature change in South Asia, where is adjacent to the northern Indian Ocean, and may release more latent heat in boreal summer. The vegetation and ocean feedbacks and the synergy between them are important for climate variability in South Asia.

The simulation results show that the vegetation feedback can be amplified by ice-albedo feedback which reflects an additional synergy in the climate system through ice glacier, therefore a more detailed feedback analysis with additional runs is warranted. It must be emphasized that the horizontal resolution in the model is too coarse to capture accurately effects of land surface changes on climate, more sensitivity experiments with mesh refinement or nesting with regional model are necessary.

Acknowledgements. This study was supported by the National Natural Science Foundation of China (NSFC) (Grant No. 40571169), the NSFC Innovation Team Project (Grant No. 40421101) and the 111 Project (Grant No. B06026). Bette Otto-Bliesner of National Center for Atmospheric Research (NCAR) is thanked for her helpful reviewing and English improvement of the manuscript.

References

An, Z. S., Porter, S. C., Kutzbach, J. E., Wu, X., Wang, S., Liu, X. D., Li, X. Q., and Zhou, W. J.: Asynchronous Holocene optimum of the East Asian monsoon, Quaternary Sci. Rev., 19, 743–762, 2000.

Berger, A. L.: Long-term variations of daily insolation and quaternary climatic changes, J. Atmos. Sci., 35, 2362–2367, 1978.

Brovkin, V., Bendtsen, J., Claussen, M., Ganopolski, A., Kubatzki, C., Petoukhov, V., and Andreev, A.: Carbon cycle, vegetation, and climate dynamics in the Holocene, Experiments with the CLIMBER-2 model, Global Biogeochem. Cy., 16(4), 1139, doi:10.1029/2001GB001662, 2002.

Casal, T. G. D., Kutzbach, J. E., and Thompson, L. G.: Present and past ice-sheet mass balance simulations for Greenland and the Tibetan Plateau, Clim. Dynam., 23, 407–425, 2004.

Chauhan, O. S.: Past 20,000-year history of Himalayan aridity: Evidence from oxygen isotope records in the Bay of Bengal, Curr. Sci. India, 84(1), 90–93, 2003.

Claussen, M., Kubatzki, C., Brovkin, V., Ganopolski, A., Hoelzmann, P., and Pachur, H.: Simulation of an abrupt change in Saharan vegetation in the mid-Holocene, Geophys. Res. Lett., 24(14), 2037–2040, 1999.

COHMAP Members: Climatic changes of the 18,000 years: Observations and model simulation, Science, 241, 1043–1052, 1988.

Christner, B. C., Mosley-Thompson, E., Thompson, L. G., and Reeve, J. N.: Bacterial recovery from ancient glacier ice, Environ. Microbiol., 5, 433–436, 2003.

Claussen, M. and Gayler, V.: The greening of Sahara during the mid-Holocene: Results of an interactive atmospheric-biome model, Global Ecol. Biogeogr., 6, 369–377, 1997.

deMenocal P., Ortiz, J., Guilderson, T., and Sarnthein, M.: Coherent high- and low-latitude climate variability during the Holocene warm period, Science, 288, 2198–2202, 2000.

Foley, J. A., Kutzbach, J. E., Coe, M. T., and Levis, S.: Feedbacks between climate and boreal forests during the Holocene epoch, Nature, 371, 52–54, 1994.

Ganopolski, A., Rahmstorf, S., Petoukhov, V., and Claussen, M.: Simulation of modern and glacial climates with a coupled model of intermediate complexity, Nature, 391, 351–356, 1998a.

Ganopolski, A., Kubatzki, C., Claussen, M., Brovkin, V., and Petoukhov, V.: The influence of vegetation-atmosphere-ocean interaction on climate during the mid-Holocene, Science, 280, 1916–1919, 1998b.

Gupta, A. K. and Anderson, D. M.: Mysteries of the Indian Ocean monsoon system, J. Geol. Soc. India, 65, 54–60, 2005.

Gupta, A. K., Anderson, D. M., and Overpeck, J. T.: Abrupt changes in the Asian southwest monsoon during the Holocene and their links to the North Atlantic Ocean, Nature, 421, 354–357, 2003.

Huang, C. C.: Environmental changes, Beijing: Science Press, 121–145, 1998 (in Chinese).

Jin, L., Ganopolski, A., Chen, F., Claussen, M., and Wang, H.: Impacts of snow and glaciers over Tibetan Plateau on Holocene climate change: Sensitivity experiments with a coupled model of intermediate complexity, Geophys. Res. Lett., 32, L17709,

doi:10.1029/2005GL023202, 2005.
Jin, L., Chen, F., Ganopolski, A., and Claussen, M.: Response of East Asian climate to Dansgaard/Oeschger and Heinrich events in a coupled model of intermediate complexity, J. Geophys. Res., 112, D06117, doi:10.1029/2006JD007316, 2007.
Kutzbach, J. E. and Guetter, P. J.: The influence of changing orbital parameters and surface boundary conditions on climate simulation for the past 18,000 years, J. Atmos. Sci., 43, 1726–1759, 1986.
Lehmkuhl, F.: Late Pleistocene, late-glacial and Holocene glacier advances on the Tibetan Plateau, Quatern. Int., 38–39, 77–83, 1997.
Lehmkuhl, F. and Oven, L. A.: Late Quaternary glaciation of Tibetan and the bordering mountains: a review, Boreas, 34, 87–100, 2005.
Maxwell, A. L.: Holocene changes inferred from lake sediments pollen and carbonate records, northeastern Cambodia, Quatern. Res., 56, 390–400, 2001.
Mayewski, P. A., Rohling, E. E., Starge, J. C., Karlen, W., Maasch, K. A., Meeker, L., Meyerson, E. A., Gasse, F. G., Kreveld, S. V., Holmgren, K., Thorp, J. L., Rosqvist, G., Rack, F., Staubwasser, M., Schneider, R. R., and Steig, E. J.: Holocene climate variability, Quatern. Res., 62, 243–255, 2004.
Molnar, P. and England, P.: Late Cenozoic uplift of mountain ranges and global climatic change: Chicken or egg?, Nature, 246, 29–34, 1990.
Morrill, C., Overpeck, J. T., and Cole, J. E.: A synthesis of abrupt changes in the Asian summer monsoon since the last deglaciation, Holocene, 13, 465–476, 2003.
Petoukhov, V., Ganopolski, A., Brovkin, V., Claussen, M., Eliseev, A., Kubatzki, C., and Rahmstorf, S.: CLIMBER-2: A climate system model of intermediate complexity. Part I: Model description and performance for present climate, Clim. Dynam., 16, 1–17, 2000.
Petoukhov, V., Ganopolski, A., Brovkin, V., Claussen, M., Eliseev, A., Kubatzki, C., and Rahmstorf, S.: CLIMBER-2: A climate system model of intermediate complexity. Part II: Model sensitivity, Clim. Dynam., 17, 735–751, 2001.
Phillips, W. M., Sloan, V. F., Sharma, P., Clarke, M. L., and Rendell, H. M.: Asynchronous glaciation at Nanga Parbat, northwestern Himalaya Mountains, Pakistan, Geology, 28, 431–433, 2000.
Prell, W. and Kutzbach, J.: Sensitivity of the Indian monsoon to forcing parameters and implications for its evolution, Nature, 360, 647–652, 1992.
Qin, D. H.: Assessment of Environmental Changes in Western China-Integration Report, Bei-

jing: Science Press, 5–6, 2002.
Ruddiman, W. F. and Kuzbach, J. E.: Forcing of late Cenozoic Northern Hemisphere climate by plateau uplift in southern Asia and the American west, J. Geophys. Res., 94, D15, 18409–18427, 1989.
Singh, I. B.: Late Quaternary evolution of Ganga Plain and proxy records of climate change, neotectonics and anthropogenic activity, Pragdhara, 12, 1–25, 2002.
Stocker, T. F., Wright, D. G., and Mysak, L. A.: A zonally averaged, coupled ocean-atmosphere model for the paleoclimate studies, J. Climate, 5, 773–797, 1992.
TEMPO Members: Potential role of vegetation feedback in the climate sensitivity of high-latitude regions: A case study at 6000 years B.P., Global Biogeochem., Cy., 10, 727–736, 1996.
Texier, D., de Noblet, N., Harrison, S. P., Haxeltine, A., Jolly, D., Joussaume, S., Laarif, F., Prentice, I. C., and Tarasov, P.: Quantifying the role of biosphere-atmosphere feedbacks in climate change: coupled model simulations for 6000 years BP and comparison with palaeodata for northern Eurasia and northern Africa, Clim. Dynam., 13, 865–882, 1997.
Thompson, L. G., Yao, T., Davis, M. E., Henderson, K. A., Mosley-Thompson, E., Lin, P. N., Beer, J., Synal, H. A., Cole-Dai, J., and Bolzan, J. F.: Tropical climate instability: The last glacial cycle from a Qinghai-Tibetan ice core, Science, 276, 1821–1825, 1997.
Thompson, L. G., Yao, T., Mosley-Thompson, E., Davis, M. E., Henderson, K. A., and Lin, P. N.: A high-resolution millennial record of the south Asian monsoon from Himalayan ice cores, Science, 289, 1916–1919, 2000.
Thompson, L. G., Mosley-Thompson, E., Davis, M. E., Mashiotta, T. A., Henderson, K. A., Lin, P. N., and Yao, T.: Ice core evidence for asynchronous glaciation on the Tibetan Plateau, Quatern. Int., 154–155, 3–10, 2006.
Tang, L., Shen, C., Liu, K. B., and Overpeck, J. T.: Changes in south Asian monsoon: new high-resolution paleoclimatic records from Tibet, Chin. Sci. Bull., 45, 87–91, 2000.
Wang, H. J.: Role of vegetation and soil in the Holocene megathermal climate over China, J. Geophys. Res., 104, 9361–9367, 1999.
Weber, S. L. and Oerlemans, J.: Holocene glacier variability: three case studies using an intermediate-complexity climate model, The Holocene, 13(3), 353–363, 2003.
Weber, S. L., Crowley, T. J., and van der Schrier, G.: Solar irradiance forcing of centennial climate variability during the Holocene, Clim. Dynam., 22, 539–553, 2004.
Yanai, M., Li, C., and Song, Z.: Seasonal heating of the Tibetan Plateau and its effects on the evolution of the summer monsoon, J. Meteorol. Soc. Jpn., 70, 319–351, 1992.

Yang, B., Brauning, A., Dong, Z., Zhang, Z., and Jiao, K.: Late Holocene monsoonal temperature glacier fluctuations on the Tibetan Plateau, Global Planet. Change, 60, 126–140, doi:10.1016/j.gloplacha.2006.07.035, 2008.

Yao, T. D., Liu, X. D., and Wang, N. L.: On amplitudes of climatic variation in Qinghai-Tibetan Plateau, Chinese Sci. Bull., 45, 98–106, 2000 (in Chinese).

Table 1. Imposed snow and glacier scenarios in modeling experiments.

Scenarios	Variations of fraction f of ice cover over the Tibetan Plateau
ICE0	f is fixed at zero for all simulations AO, AV, AOV (grey line in Fig. 1a)
ICE1	linearly increasing for the 9 kyr-transient simulation, starting with 0 at 9 kyr BP and ending with 0.2 at 0 kyr BP (green line in Fig. 1a)
ICE2	linearly increasing by 0.05 (1/4 of the maximum of fractional ice cover at 0 kyr BP as in ICE1) during four periods including 7.2–8.2 kyr BP, 4.9–5.8 kyr BP, 2.4–3.32 kyr BP and 3.0–4.5 kyr BP, and fixed with the values the previous period reached maximum during other periods, which are mainly based on result in work of Lehmkuhl (1997) (purple line in Fig. 1a)
ICE3	linearly and slightly increasing in the early Holocene (9–7 kyr BP), starting with 0 at 9 kyr BP and reaching to 0.017 at 7 kyr BP, then prescribed linearly and rapidly increasing in the mid-Holocene (7–5 kyr BP), reaching to 0.117 at 5 kyr BP, finally prescribed linearly and slightly increasing between 5 and 0 kyr BP, ending with 0.2 at 0 kyr BP, which mimic the Nigardsbreen Glacier (62° N,7° E) expansion during the Holocene (reference results from a process-based glacier model coupled to the intermediate-complexity climate model (ECBilt), Weber et al., 2003) (red line in Fig. 1a)
ICE4	linearly increasing between 9 and 6 kyr BP, starting with 0 at 9 kyr BP and reaching to the maximum 0.2 at 6 kyr BP, then fixed at 0.2 between 6 and 0 kyr BP, which mimic Abramov glacier (40° N, 72° E) variation during the Holocene resulted from ECBilt (Weber et al., 2003) (blue line in Fig. 1a)

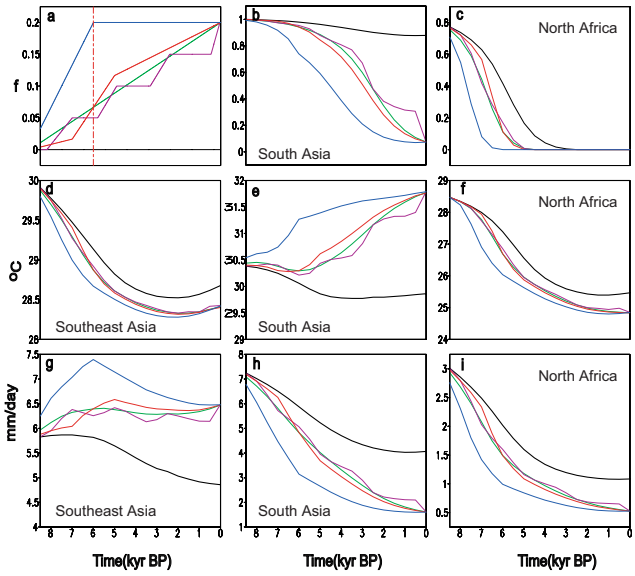

Fig. 1. Transient simulation using CLIMBER-2 for the last 9 kyr. **(a)** Prescribed various scenarios of snow and glaciers developing over the Tibetan Plateau in transient simulation (f: fraction of snow and glaciers); **(b)** Simulated changes of fraction f of vegetation cover in South Asia (40° E–95° E, 20° N–30° N) in simulation AOV with different imposed ice scenarios in (a); **(c)** Same as (b) but for North Africa (15° W–40° E, 20° N–30° N); **(d)** Same as (b) but for summer (June, July, August, JJA) near-surface air temperature in Southeast Asia (95° E–145° E, 20° N–30° N); **(e)** Same as (d) but for South Asia (40° E–95° E, 20° N–30° N); **(f)** Same as (e) but for North Africa; **(g)** Same as (f) but for JJA precipitation in Southeast Asia; **(h)** Same as (g) but for South Asia; **(i)** Same as (h) but for North Africa. Colors indicate different imposed ice scenarios ICE0 (no ice) (grey), ICE1 (green), ICE2 (purple), ICE3 (red), and ICE4 (blue), respectively, in transient simulation AOV. The vertical red dash line indicates mid-Holocene (6 kyr BP) in Fig. 2.

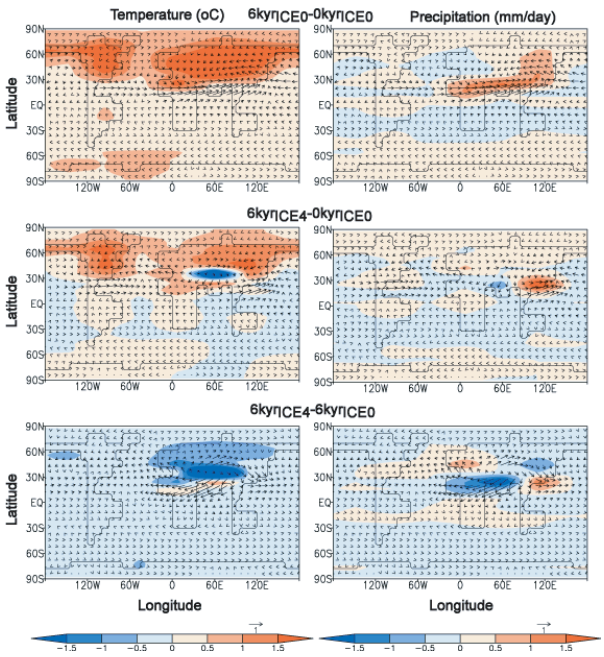

Fig. 2. Boreal summer near-surface air temperature (°) (left panel) and precipitation (mm/day) (right panel) differences between mid-Holocene (6 kyr BP) and 0 kyr BP simulations for different imposed ice scenarios. (6 kyr_{ICE0}–0 kyr_{ICE0}) indicates mid-Holocene (6 kyr BP) minus present day (0 kyr BP) simulations for scenario ICE0 (no-ice), (6 kyr_{ICE4}–0 kyr_{ICE0}) indicates 6 kyr BP simulation for scenarios ICE4 minus 0 kyr BP simulation for scenario ICE0 and (6 kyr_{ICE4}–6 kyr_{ICE0}) indicates 6 kyr BP simulation for scenarios ICE4 minus 6 kyr BP simulation for scenarios ICE0. Vector arrows indicate simulations of 850 hPa wind field (m/s) differences between 6 kyr BP and 0 kyr BP for corresponding imposed ice scenarios.

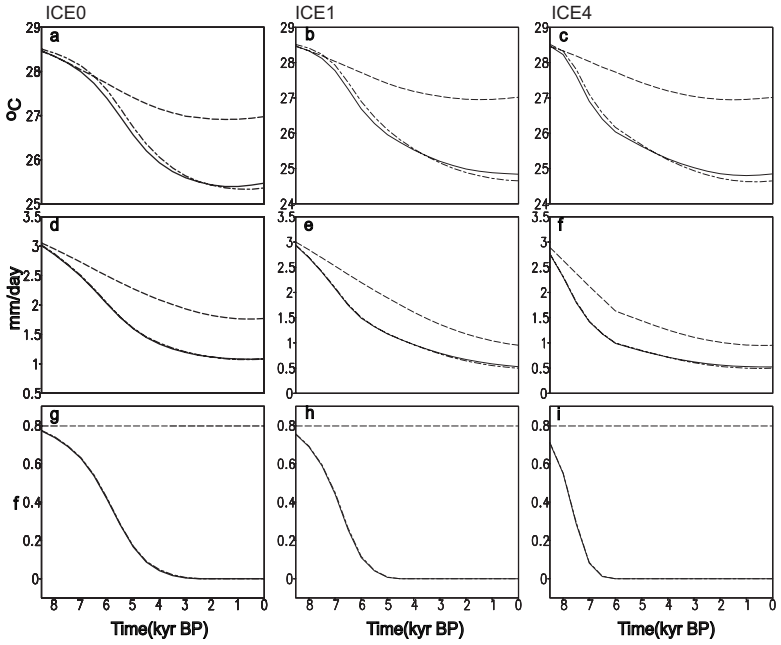

Fig. 3. (a) Summer (June, July, August, JJA) near-surface air temperature (a, **b**, **c**), precipitation **(d, e, f)**, and vegetation cover **(g, h, i)** changes in North Africa (15° W–40° E, 20° N–30° N) for the last 9 kyr in simulations AO (long dash line), AV (long and short dash lines), and AOV (solid line) with imposed ice scenarios ICE0 (no-ice) (a, d, g), ICE1 (b, e, h), and ICE4 (c, f, i).

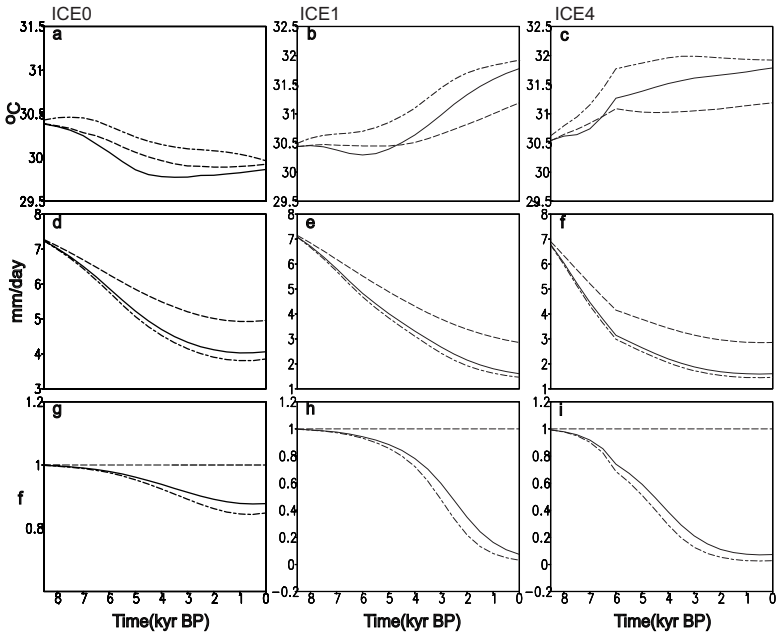

Fig. 4. Same as Fig. 3 except for regions in South Asia (40° E–95° E, 20° N–30° N).

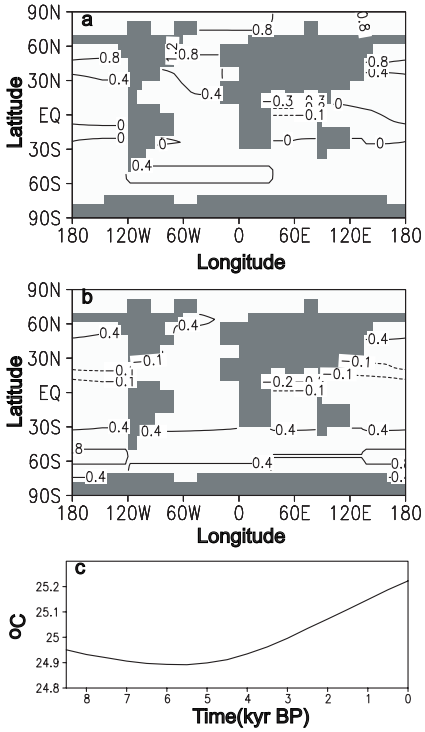

Fig. 5. Differences in sea surface temperatures (SSTs) between 9 kyr BP and 0 kyr BP in simulation AOV without imposed ice cover over the Tibetan Plateau (scenario ICE0) in boreal summer **(a)** and winter **(b)**; **(c)** boreal summer SST changes in North Indian Ocean (40° E–95° E, 0° N–20° N) for the last 9 kyr in simulation AOV with scenario ICE0.